Microfluidics and Nanofluidics (2022) 26:22
https://doi.org/10.1007/s10404-022-02520-8

RESEARCH PAPER

Microfluidic paper-based analytical device (μPAD) fabricated by wax screen printing technique for the determination of nitrite and nitrate ion in water samples

Tilaye Tesfaye[1] · **Ahmed Hussen**[1]

Received: 12 May 2021 / Accepted: 1 January 2022 / Published online: 27 February 2022

Abstract
A microfluidic paper-based analytical device (μPAD) is a new technology platform for extremely low-cost sensing applications. This study aimed to explore for an inexpensive alternative fabrication method. Accordingly, a simple wax screen printing fabrication manageable with locally available materials has been elaborated and successfully demonstrated for the determination of nitrite and nitrate ion(s) in water samples. The operational parameters such as sample and Griess reagent volume, color development time, and zinc powder loading were optimized. Applying the optimal conditions, the limits of detection for nitrite and nitrate ion were found to be 0.16 and 0.87 ppm, respectively. The level of sensitivity observed in μPAD is adequate to determine the threshold concentration limit for nitrite (1 ppm) and nitrate (50 ppm) in drinking water set by WHO. The μPAD revealed 95% recovery compared with the standard method UV–vis spectrophotometry (> 96%), which indicates the validity of the developed method. Furthermore, the application of μPADs and UV–vis spectrophotometry for the analysis of Dire Dawa groundwater samples showed below the detection limit for nitrite. In contrast, 71 ppm of nitrate concentration was found in the ground water by using both methods. The concentration measured using μPADs was in an excellent agreement with the values obtained from UV–vis spectrophotometry. This implies a potential use of the μPADs for environmental monitoring of nitrate and nitrite in resources limited areas without the need for expensive benchtop analytical devices.

Keywords μPADs · Nitrate · Nitrite · Griess reagent · Wax screen-printing · Colorimetric detection

1 Introduction

Nitrate and nitrite are the most prevalent contaminants of the aqueous environment and serve as significant indicators of natural water quality (Mikuška and Večeřa 2003; Rezaee et al. 2008). For many years, these ions have been associated with cancer, especially nitrite, either from direct ingestion, or the nitrate reduction by bacteria in human saliva (Ferreira et al. 2020; Ward et al. 2018). Ingestion of nitrate from contaminated source can be reduced into nitrite by oral bacteria. When nitrite reaches the acidic environment of the stomach and combined with amine or amide, it forms nitrosamines and nitrosamides. These compounds are known to be toxic and carcinogenic, thus contributing mainly to the development of gastric cancer and blue baby syndrome (van Breda et al. 2019; Ward et al. 2018). The nitrites in the bloodstream could transform hemoglobin to methemoglobin by oxidation of ferrous iron (Fe^{2+}) in hemoglobin to ferric form (Fe^{3+}) preventing or reducing the ability of blood to transport oxygen, which causes cyanosis and anoxemia (Bruning-Fann and Kaneene 1993). Due to these potential hazardous effects, the US EPA set maximum acceptable concentration (MAC) level for nitrite and nitrate in drinking water to be 1.0 and 10.0 mg/L, respectively (Acrylamide 2009). Therefore, to ensure environmental safety, it is important to monitor the levels of nitrite and nitrate in food and drinking water.

Different analytical instruments that have been used to measure nitrate and nitrite include ion chromatography (Chiu et al. 2007), sequential injection analysis (Pistón et al. 2011), capillary electrophoresis (Kostraba et al. 1992), electrochemical techniques (Bhatnagar and Sillanpää 2009),

✉ Ahmed Hussen
ahmed.hussen29@aau.edu.et

[1] Center for Environmental Science, College of Natural and Computational Sciences, Addis Ababa University, PO Box 1176, Addis Ababa, Ethiopia

and UV–vis spectrophotometry (Narayana and Sunil 2009). These instruments are known to be expensive and require a high level of training to operate reliably. The world health organization (WHO) also set a policy direction that diagnostic and health hazard monitoring devices for developing countries should be ASSURED: affordable, sensitive, specific, user-friendly, rapid and robust, equipment-free and deliverable to end-users (Martinez et al. 2010). Therefore, it is indispensable to explore for simple analytical devices that could be used for regular monitoring of target analytes particularly in resource-limited set-up.

Microfluidic paper-based analytical devices (μPADs) have gained increasing interest as simple, low cost, and portable analytical tools. The fundamental principle in the fabrication of μPADs is to pattern a sheet of paper into hydrophilic sample port, channels, and detection zones bounded by hydrophobic barriers to create micro-scale capillary channels on the paper. The pattern is usually generated by depositing wax as hydrophobic material on the paper to guide the liquid wicking through the hydrophilic portion. Recently, polylactic acid (Teepoo et al. 2019) and natural beeswax (Thongkam and Hemavibool 2020) have been used to create the hydrophobic barrier for the μPAD determination of nitrite and nitrates. Several techniques have been used for μPAD fabrication in the analysis of nitrite including photolithography (Klasner et al. 2010), inkjet printing (Jayawardane et al. 2014), wax printing (Bhakta et al. 2014; Charbaji et al. 2021a, b; Ratnarathorn and Dungchai 2020; Trofimchuk et al. 2020), stamping method (Cardoso et al. 2015), paper cutting (Ortiz-Gomez et al. 2016), electrokinetic stacking (Zhang et al. 2018) and screen printing method (Teepoo et al. 2019; Thongkam and Hemavibool 2020). Most of the aforementioned fabrication methods demand for tools/devices that are not easily accessible in laboratories of developing countries. For instance, photolithography needs expensive reagents, photomask and UV light, wax printing demand wax printer whose production has been discontinued by Xerox and associated consumables, inkjet printer needs customized inkjet printer (Nishat et al. 2021).

On the other hand, wax screen-printing method is an easy-to-use and inexpensive alternative fabrication method for μPAD, which will be especially useful in developing countries (Dungchai et al. 2011). It can be managed with simple materials such as transparency, nylon screen, solid wax and dryer. It doesn't require a special device as compared with most of the fabrication methods mentioned above. However, only two studies have been conducted by screen printing fabrication for nitrite and nitrate determination. Thongkam and Hemaviabool (2020) reported that under optimal condition the beeswax screen printing method provides a well-defined hydrophobic barrier with an efficient resolution, good reproducibility and low detection limit (0.1 and 0.4 ppm for nitrite and nitrate, respectively) while the polylactic acid screen printing method (Teepoo et al. 2019) resulted in a higher limit of detection; 1.2 and 3.6 ppm for nitrite and nitrate, respectively. As μPAD is an emerging platform, more basic research is still required to demonstrate alternative simple fabrication methods and analytical capabilities of the technology. In the present work, a simple home-made wax screen-printing method has been used for the fabrication of μPADs in our laboratory. Besides, various parameters were optimized for the colorimetric determination of nitrate and nitrite in real and synthetic water samples, and the method was validated using UV-vis spectrophotometry. Under the optimum conditions, we have obtained a limit of detection (0.16 and 0.87 ppm for nitrite and nitrate, respectively) much better than the previously reported polylactic acid screen printing method.

2 Materials and methods

2.1 Chemicals and equipment

Spectral measurements were carried out using a UV–vis spectrophotometer (HACH DR600). Light microscope (OMAX, M82ES) and electronic balance were used to identify the boundary of the hydrophilic hydrophobic region and for weighing the chemicals, respectively. Whatman Filter paper no. 1, micropipettes (dragon, Germany), iPhone 5S tablet, Hairdryer (2000watts), wooden frame (21 cm × 30 cm), mesh (57 μm), solid wax, squeegee, adhesive tape, transparency film were purchased from local market. The following chemicals were used to conduct the experimental work: Fotolack TR-88 and diazo F sensitizer (Feteks, Turkey); Sulfanilic acid (99%), glacial acetic acid and zinc dust (95%) from Loba Chemie, India; *N*-(1-naphthyl)-ethylene diammonium dichloride (Sigma Aldrich, Germany); potassium nitrate (99%) (BLULUX, India); 99% purity sodium nitrite, potassium chloride and sodium acetate from UNI-CHEM.

2.2 Development of patterned paper-based device

The wax screen-printing method described by Dungchai et al. 2011 and Namwong et al. 2018 was customized and the set-up for fabrication was modified using locally available materials. The fabrication process can be categorized into two phases: (1) printing the design on the mesh screen and (2) transferring the design from the mesh to the filter paper. Each phase involves a series of steps that have been described as shown in Fig. 1. Circular zones (1 cm diameter) were designed using Microsoft PowerPoint 2016 and printed on a transparency using a laser printer (Fig. 1A). Black areas on the transparency are used to generate a hydrophobic area on the paper, while colorless areas yield hydrophilic zones.

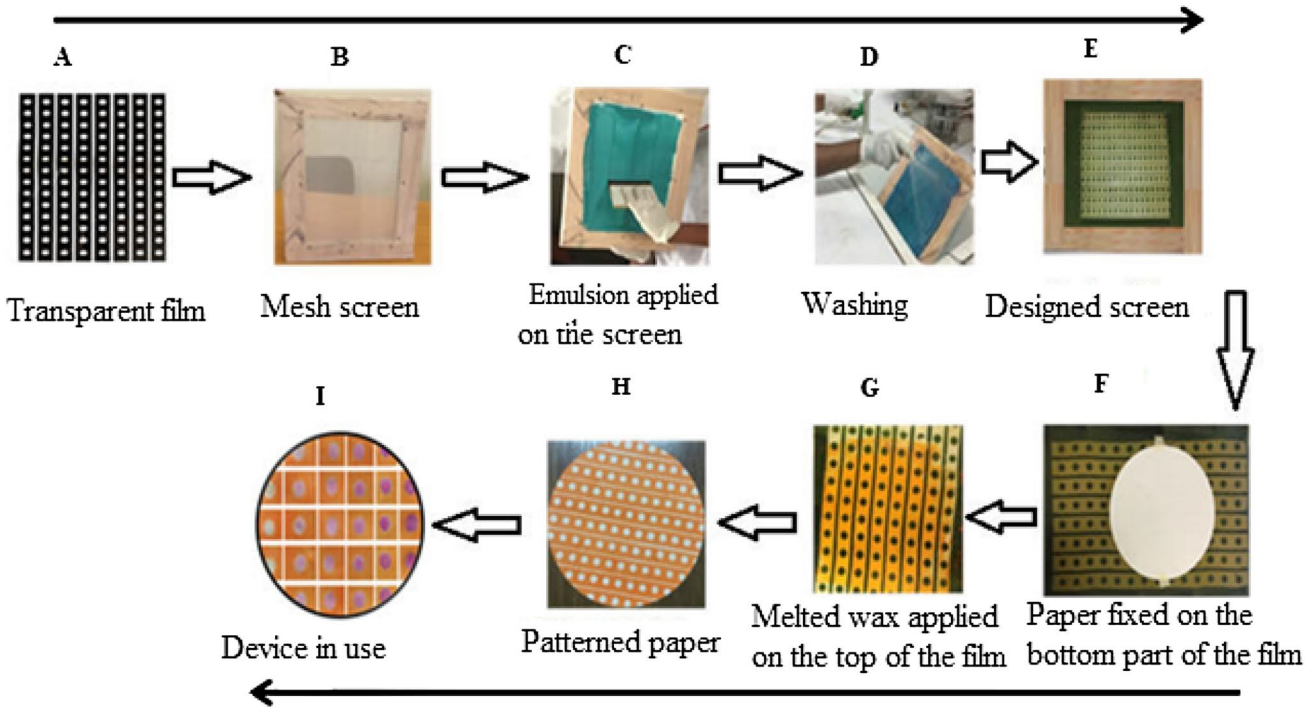

Fig. 1 The process of fabricating the device

A fine mesh of size 57 µm was stretched on a wooden frame (Fig. 1B). An emulsion was prepared by mixing 40 mL of fotolack TR-88 with 5 mL of diazo F sensitizer and left for 12 h in a dark room. The emulsion was applied on both sides of the mesh stretched on a wooden frame (Fig. 1C) and dried in a dark box to keep away from light. After drying the emulsion, the transparency film was placed over the coated screen and then exposed to a fluorescence light source (2500 lx) at a distance of 30 cm. The fluorescence light passes through the clear areas (circular zones) and induces a polymerization (hardening) of the emulsion. The area of the emulsion that is exposed to light hardens, so blocking the screen (circular zones) which will be used for creating a hydrophilic part on the paper. The part protected from light by the opaque areas (black part) remains soluble and washed away with pressurized water opening the mesh for creating the hydrophobic part on the paper (Fig. 1D). Eventually, by this process, the design is printed on the mesh screen (form a film on a mesh) and ready to be used for the fabrication of the µPADs (Fig. 1E).

To fabricate the µPAD, a filter paper was put on the bottom of the patterned screen (Fig. 1F) and the melted solid wax (at 60 °C for 10 min) was applied to the patterned screen from the top and squeegeed to insert the melted wax into the screen (Fig. 1G). The melted wax passed through the screen onto the paper creating a hydrophobic barrier on the paper but can't pass through the black spots which remain as white hydrophilic zones of reaction (Fig. 1H). The paper was separated from the mesh screen by blowing with a home hair dryer (power of 2000 watts) and before use a clear packing tape was put on the backside of the patterned paper to prevent leaking during the analysis. The white zones are where the chromogenic reagents are loaded and a colorimetric reaction takes place (Fig. 1I) with the analyte of interest.

2.3 Preparation of stock solution and reagent

Griess reagent was prepared as described by Pereira et al. (2012). It was synthesized by mixing an equal ratio of sulfanilamide and *N*-(1-naphthyl) ethylene diamine (NED) solutions. Sulfanilamide reagent was prepared by dissolving 600 mg of sulfanilic acid in 50 mL of hot water. After cooling the mixture at room temperature, 20 mL of glacial acetic acid was added to the mixture and diluted to 100 mL with deionized water. NED reagent was prepared by dissolving 20 mg of *N*-(1-naphthyl)-ethylene diammonium dichloride

(NEDD) in 20 mL of glacial acetic acid and the mixture was diluted to 100 mL with deionized water (Pereira et al. 2012). NED and sulfanilamide solutions were prepared separately, this helped to extend the shelf-life time of the Griess reagent.

UV–vis spectrophotometry was used to characterize the Griess reagent prepared in the laboratory. The Griess reagent (1 mL) was added to 10 mL of 1 ppm nitrite solution to form an azo-dye complex. The azo-dye complex was scanned using UV–vis spectrophotometry in the range of 200–700 nm to obtain the wavelength of maximum absorption.

A 500 mL of 100 mg/L stock solution of sodium nitrite was prepared by dissolving 0.246 g of pre-dried (at 105 °C for 4 h) powder in a volumetric flask using distilled water. Stock nitrate solution (100 mg/L) was prepared by quantitatively transferring 0.180 g of pre-dried (105 °C for 4 h) potassium nitrate to a 250 mL volumetric flask containing approximately 200 mL of distilled water and diluted to the mark. Working nitrite solutions were prepared fresh on daily basis.

Nitrite ion can be directly detected with the Griess reagent; however, for the determination of nitrate ion, zinc powder was used to reduce nitrate to nitrite (Murray et al. 2017). Griess reagent was deposited on the paper device and allowed to dry for 10-min, followed by adding a drop of sodium nitrite solution to complete the azo-dye complex formation (pinkish color). The developed color of the azo-dye complex was captured using an iPhone 5S tablet camera and the corresponding color intensity was inverted and analyzed as weighted average intensity of the RGB color using ImageJ software. In all the cases a circular region of interest (ROI, 6500 pixels) was selected around each detection zone for color intensity measurement.

2.4 Optimization of major parameters for colorimetric determination

2.4.1 Reagent volume

The holding capacity of the hydrophilic region of the μPAD was evaluated by dropping different volumes (1, 2, 3, 4, 5, and 6 μL) of red food dye using a micropipette. Furthermore, the effect of Griess reagent volume (1–5 μL) on the paper device was investigated. Griess reagent (1 μL) was dropped onto 5 wells of paper-based devices containing different concentrations of nitrite solution (0, 1, 2, 4, and 6 ppm). Similarly, the effect of Griess reagent volumes (2, 3, 4, and 5 μL) were investigated separately for each of the five concentration levels. Fully developed colors were captured using an iphone5 camera and the corresponding weighted average intensity of RGB color were inverted and analyzed using ImageJ software. Finally, the optimal volume of a Griess reagent was obtained from a graph plotted as a function of Griess reagent volume versus mean gray intensity.

2.4.2 Sample volume

The volume of the sample was optimized by using the optimal volume of Griess reagent. Different sample volumes of 1, 2, 3, 4, and 5 μL of different concentration (0, 1, 2, 4, 6, and 8 ppm) of nitrite solution were added to each reaction well that contained the optimal reagent volume. The mixture was then allowed to dry at room temperature. The image developed was inverted and analyzed as weighted average intensity of the RGB color using ImageJ software. Finally, the graph of mean gray intensity versus volume of sample was constructed.

2.4.3 Time needed for the formation of azo-dye complex

The time needed for complete formation of azo-dye complex was optimized by capturing a picture of the developed color at a different time range. Each triplicated hydrophilic zone was spotted with 1 μL of color- forming reagent (a mixture of sulfanilamide and NED) and allowed to dry at room temperature in a dark box for 10 min (Cardoso et al. 2015). Then, 5 μL of 1 ppm nitrite sample solution was added into the reagent to form azo- dye complex. The developed colors were captured every 5 min starting from 2 min of reaction time up to 45 min. The captured photos were analyzed as weighted average RGB color intensity values using ImageJ software.

2.4.4 Amount of zinc powder required for nitrate ion determination

The optimal quantity of Zn powder was determined in both μPAD and UV–vis spectrophotometry methods. In the former method, Zn powder ranging from 2.5 to 12.5 mg was added to the sample solution containing a mixture of 2.5 mL (10 mg/L NO_3^-) standard solution and 1 mL Griess reagent. In the latter method, Zn powder (10–250 mg) was added to the sample solution containing a mixture of 10 mL (10 mg/L NO_3^-) standard solution and 1 mL Griess reagent. Each sample was shaken and allowed to stand for 5 min to complete the reduction reaction and the color intensity and absorbance were measured.

2.5 Analytical features for the method

2.5.1 Linearity

Linearity was evaluated for nitrite and nitrate concentration in the range of 0.4–2 ppm and 1–10 ppm, respectively. A 1 μL of Griess reagent was dropped

onto a paper-based device ($n = 3$) and 5 µL of nitrite solution (different concentrations) was pipetted onto the device. The color intensities were analyzed using ImageJ software. The data were plotted as mean gray intensity versus nitrite concentration. Similarly, in the UV–vis spectrophotometry, linearity was evaluated in the range of 0.1–1.4 mg/L and 0.5–12 mg/L for nitrite and nitrate, respectively.

2.5.2 Limit of detection

The limit of detection (LOD) is the lowest analyte concentration likely to be reliably distinguished from the blank. In this work, experimental LOD was evaluated as the lowest nitrite concentration that can give measurable signal. The LOD for both UV–vis spectrophotometry and µPADs techniques was calculated based on the regression line as *y*-intercept plus three times the standard error (Sy/x) of the signal (intensity/absorbance in the *y*-direction). Similarly, limit of quantitation (LOQ) as y-intercept plus ten times the standard error (*Sy*/*x*). The standard error (Sy/x) of the signal is obtained from the Excel regression output (Miller and Miller 2018).

2.5.3 Interference studies

Some common ions that interfere with nitrite and nitrate ion determination were considered in this study. Different concentrations of KCl and CH_3COONa were introduced into the sample solutions as a precursor for the interfering anions (Cl^- and CH_3COO^-). The standard solutions containing 1 ppm nitrite and 10 ppm nitrate was exposed to the concentration levels of 50–1000 ppm of KCl and CH_3COONa. The effect was monitored by analyzing percentage recovery of the nitrite and nitrate using µPAD analysis.

2.6 Method validation

The validity of the proposed method was evaluated using the standard addition method. For this purpose, known amounts of standard nitrite were spiked to tap water and the total amount of the analyte was estimated by both µPAD and UV–vis spectrophotometry. Tap water samples collected from Addis Ababa University, science faculty campus, was used for method validation. Samples were collected by using polyethylene plastic containers. The tap water was allowed to run for at least 20 min before sample collection. Three samples of replicates were collected from the three locations (near a digital library, around the student cafeteria, and near the graduate building) and mixed to take representative samples. The collected samples were stored at 4 °C in a refrigerator and analyzed within 48 h after collection to obtain reliable nitrite concentration.

2.7 Real sample analysis

To evaluate the performance of the µPADs, borehole water samples were collected in a pre-cleaned plastic container from Dire Dawa city (347 km from Addis Ababa) with the help of Dire Dawa city water supply and sanitation authority. The composite samples were collected from different wells and stored at 5 °C in the icebox and transported to Addis Ababa University, Center for Environmental Science laboratory and kept in a refrigerator until the time of analysis.

Direct analysis of the groundwater sample for nitrate revealed a huge intensity/absorbance that goes beyond the calibration curve. This implies that the groundwater samples contained a very high concentration of nitrate which demands dilution for quantification within the calibration curve. Accordingly, 5 mL of groundwater sample was taken and diluted to a 50 mL total volume using distilled water. After reduction with zinc powder, the nitrate was quantified using µPADs and UV–vis spectrophotometry.

3 Results and discussion

3.1 Characterization of printed microfluidic channels in the paper

The reproducibility in the size of the hydrophilic zone is very important as this region is where the chemical reaction is taking place. Its size plays an important role to miniaturize the reagent and sample volume. So, the reproducibility of the device was evaluated by measuring the inner zone diameter of the hydrophilic circle using a Vernier caliper. The average diameter of 50 circular micro-zones was 9.00 ± 0.02 mm, indicating a good fabrication reproducibility of the screen-printing method.

From the food dye solution drop test, the optimal holding capacity of the circular spot (reaction wells) was found to be 6 µL. This will be dictating the volume of chromogenic reagents and samples to be introduced in the detection zone. The water-resistance of the wax applied to the paper was evaluated to check the effectiveness of the hydrophobic barriers. The light microscope image result (Fig. 2A), clearly shows the porosity of the fiber part of the cellulose (hydrophilic paper), which helps to hold chemicals for the reaction. However, on the hydrophobic region (wax applied part), the fiber part of the cellulose was blocked by the melted wax. When applying the same volume of aqueous food dye solution on the hydrophilic and hydrophobic regions of the filter paper (Fig. 2B), the hydrophobic part didn't get wet by the aqueous solution

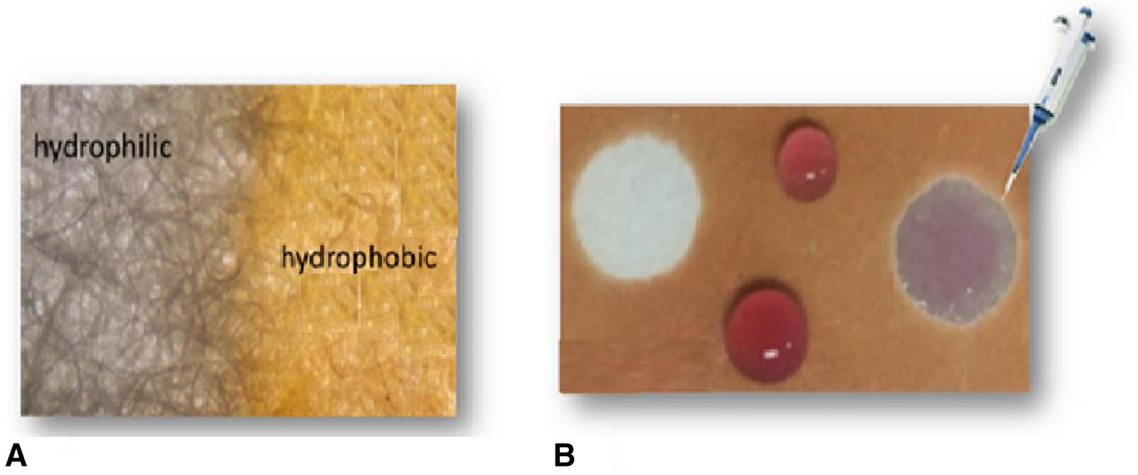

Fig. 2 **A** The hydrophilic and hydrophobic barrier of the device using light microscope image with the magnification of × 40. **B** The difference between a hydrophilic (white spot) and hydrophobic part (orange) response to a drop of food dye solution

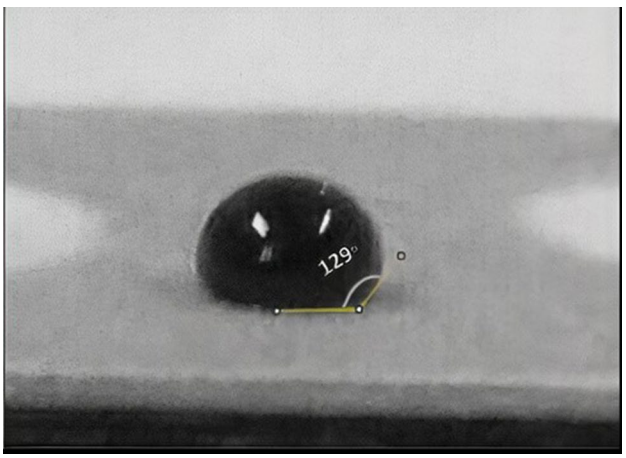

Fig. 3 Contact angle approximation

and the drop recoils (it remains intact as droplets), in contrast, the same volume of the food dye solution was absorbed and spread in the hydrophilic zone. Another evidence for the efficient formation of the hydrophobic barrier comes from contact angle measurement. If the solid surface is hydrophobic, a contact angle greater than 90° is well established in several studies. For instance in the work of Teepoo et al. (2019), a 9% concentrations of polylactic acid as a hydrophobic barrier gave a water contact angle of 117°. As it can be seen from Fig. 3, a wax modified filter paper surface showed a food dye solution contact angle of 129°. This clearly shows that the hydrophobic wax penetrates throughout the thickness of the filter paper and hence effectively blocks the flow of the aqueous solution within the hydrophilic region.

3.2 Factors affecting colorimetric assay

3.2.1 Reagent volume

The volume of both Griess reagent and nitrite solution added to the hydrophilic paper zone were optimized. Figure 4A displays the color intensity variation with respect to the change in the concentration of nitrite (0–6 ppm) and volume of Griess reagent (1–5 µL). The color change from one concentration level to the other can be easily observed by our naked eye.

Furthermore, a plot of the volume of the reagent versus intensity at a specific concentration (1 ppm) was also made to get the optimal Griess reagent volume required (Fig. 4B). As can be seen in Fig. 4B, all volumes of the Griess reagent (1–5 µL) gave color intensity ranging from 103 to 105. Almost similar color intensity results were observed irrespective of the volume of reagent used. Statistical analysis of the data using one-way ANOVA (at 5% probability) also confirmed that there is no significant difference (P value of $0.868 > 0.05$) in the intensity by varying the volume of the reagent at specific concentration. This implies that 1 µL of Griess reagent is adequate for the colorimetric assay of nitrite and nitrate.

3.2.2 Sample volume

To check the effect of sample volume on color intensity, the sample volume of nitrite solution was optimized in the range 1–5 µL at constant reagent volume (1 µL) and various concentrations of nitrite (0–8 ppm). Figure 5 shows that an increase in the sample volume resulted in color intensity enhancement in the reaction zone.

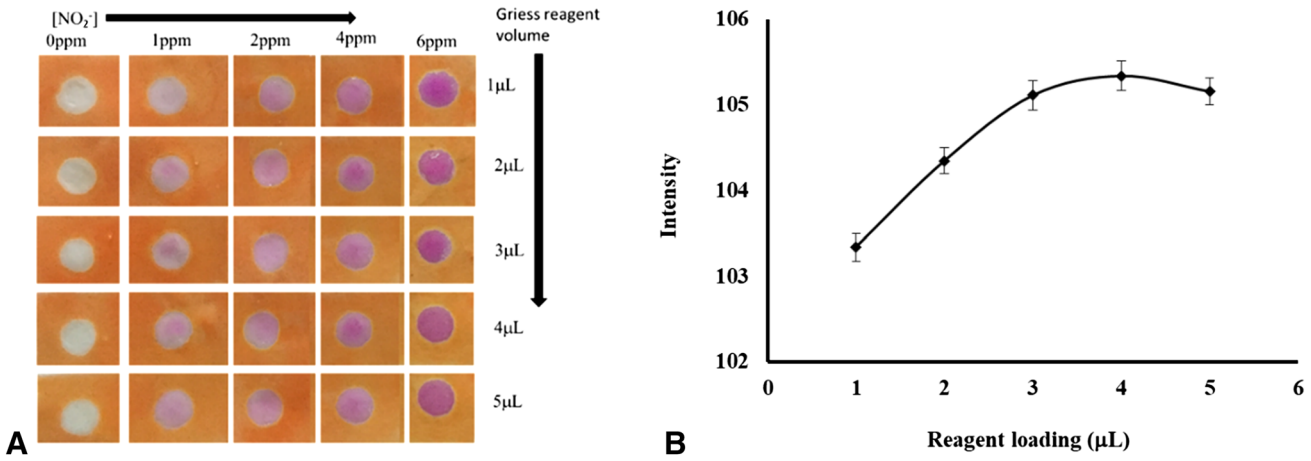

Fig. 4 **A** Intensity variation with respect to change in $[NO_2^-]$ and volume of Griess reagent **B** Gray intensity versus change in volume of Griess reagent at 1 ppm $[NO_2^-]$ ($n=3$)

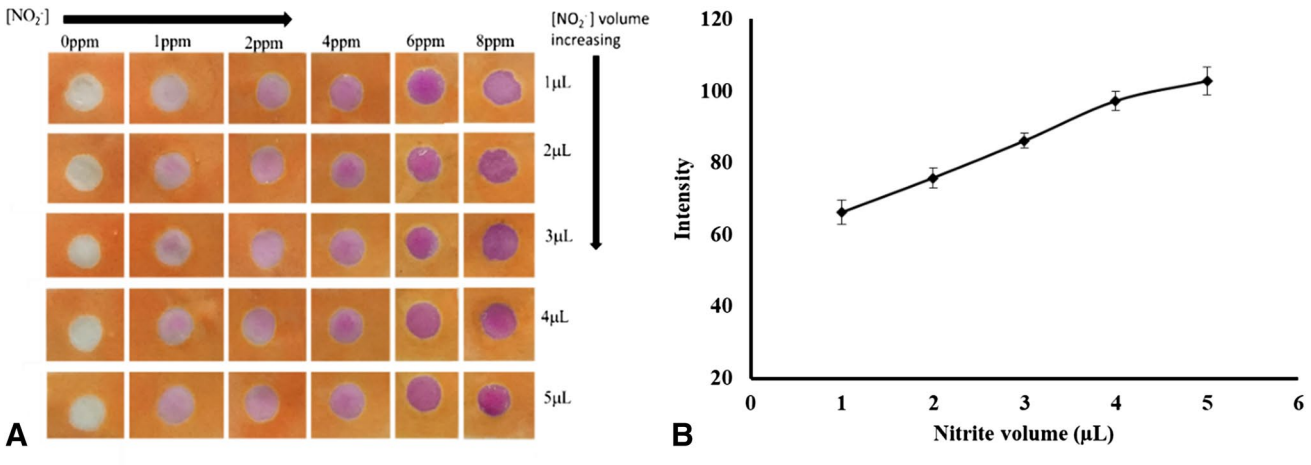

Fig. 5 **A** Intensity variation with respect to change in concentration $[NO_2^-]$ and volume of NO_2^-. **B** Gray intensity versus volume change at 1 ppm $[NO_2^-]$ ($n=3$)

In a given concentration, the difference in the intensities with respect to variation in analyte volume can't be realized by our naked eye. However, the difference can be easily noticed from the color intensity measurement results shown in Fig 5B. Figure 5B displays a plot of gray intensity versus volume of nitrite at a concentration of 1 ppm, which shows intensity increment with the volume of nitrite. Similarly, an increasing trend in intensity with volume, has been observed at other concentration levels as well. One way ANOVA analysis showed statistically significant differences in the mean intensities by varying the volume of sample (P value of 2.18E−07 < 0.05). The least significance difference (LSD) applied as post hoc analysis also revealed that all the intensities are significantly different. As can be seen in Fig 5B, the color intensity obtained at 5 µL (103) is significantly higher than that of the intensity at 4 µL (97). This indicates that at 4 µL volume the reaction is not complete, there are still some unreacted Griess reagents remaining for further reaction with nitrite. Therefore, a sample volume of 5 µL was used as an optimum volume of the sample for this assay. Higher volumes of the sample were not studied because the total volume added to the paper device (the sum of the volume of reagent and the sample) is dictated by the holding capacity of reaction wells (circle) which is 6 µL.

3.2.3 The azo-dye complex stability

The color of the azo-dye complex was monitored at ambient temperature (20−25 °C) by recording the intensity every 5 min once it is formed (within 2 min). The azo dye complex intensity was 99, 104, and 103 after 5, 10, and 15 min of

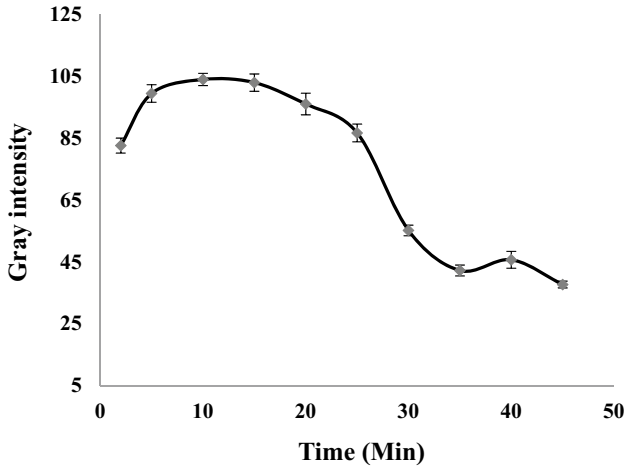

Fig. 6 Azo-dye complex stability variation with time ($n=3$)

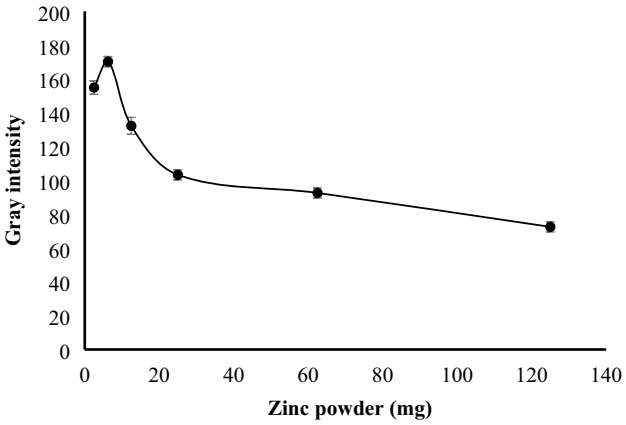

Fig. 7 A plot of zinc loading versus intensity in µPADs ($n=3$)

the complex formation, respectively (Fig. 6). The ANOVA single factor test indicates that there is no significant difference in the intensity of the azo dye complex within 5–15 min at 95% confidence level. This implies that the azo-dye complex formed has a very good stability from 5 to 15 min. However, after 15 min, the intensity of the azo-dye complex is gradually decreasing, which indicates the decomposition of the complex (Limousy et al. 2010). Therefore, the azo-dye color intensity which is the basis for colorimetric quantification should be measured within 5–15 min.

3.2.4 The amount of zinc powder

The nitrate ion is not directly determined using Griess reagent; it has to be reduced to nitrite using various reducing agents. Among this potential reducing agents zinc powder was selected for this specific study. Initially an attempt was made to use a µ-PAD design containing a separate treatment zone for loading zinc before the detection zone, which is different from the paper microzone being used in this study. However, in that approach zinc particles are not held in place and swept into the detection zone by the flowing sample without sufficiently reducing nitrate; hence leads to underestimation of the nitrate. Therefore, in the present work, the amount of zinc powder required for the complete reduction of nitrate was separately optimized before introducing the samples to µ-PAD system. As shown in Fig. 7, when 2.5 mg of zinc was initially used, low intensity was observed implying that the nitrate in the sample is not fully reduced to nitrite ion. The intensity starts to increase with increasing mass of zinc to 6.25 mg (optimum value) and after that, it decreases. In using UV–vis spectrophotometry, a similar pattern was observed for the plot of absorbance versus zinc loading. The decreasing trend in intensity/absorbance after optimum value was probably due to more quantities of zinc powder used which might cause the over reduction of nitrite to lower oxidation states such as ammonia. Furthermore, higher quantities of zinc powder form turbidity and consequently decrease the intensity/absorbance value when it is analyzed using ImageJ software/UV–vis spectrophotometry.

Besides mobility, other problems associated with zinc deposition includes lack of repeatability in the amount deposited and uniform surface distribution (Charbaji et al. 2021a, b). To address these limitations, recently Charbaji et al. 2021a, b reported the use of zinculose, a composite material of cellulose fibers with embedded zinc microparticles, in a paper-based microfluidic device for converting nitrate to nitrite. The authors claim 36% enhancement in the conversion compared with the direct zinc loading in the paper channel.

3.3 Analytical performance of the method

3.3.1 Calibration curves

The calibration curve was constructed using a standard solution of nitrite in the concentration range of 0.4–2.0 mg/L under optimized conditions. As shown in Fig. 8A, the calibration curve obtained using µPADs has a good linearity with a correlation coefficient (R^2) value of 0.9931. The calibration curve for nitrite ion was also studied using UV–vis spectrophotometry and good linearity ($R^2 = 0.995$) was observed in the range of 0.1–1.4 mg/L (Fig 8B). Similarly, for the nitrate ion, calibration curves with correlation coefficient (R^2) of 0.9934 and 0.9956 were observed by using µPADs and UV–vis spectrophotometry, respectively.

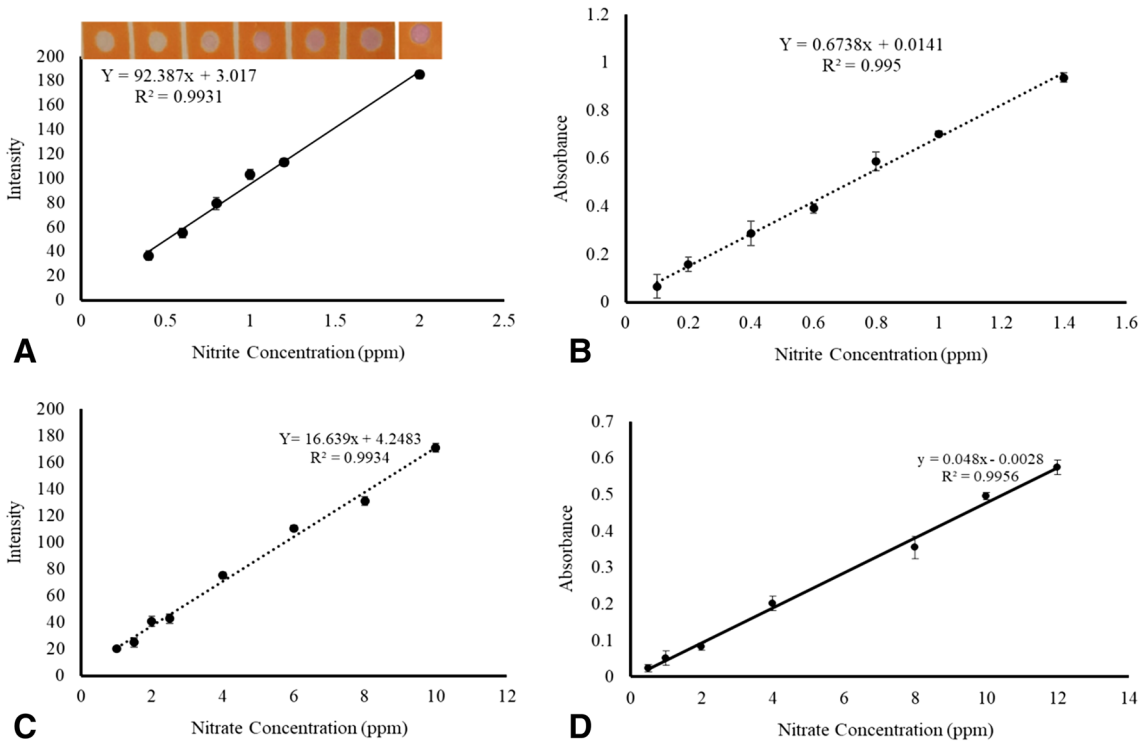

Fig. 8 Calibration curve for nitrite and nitrate ($n = 3$) using µPADs (**A, C**) and UV–vis spectrophotometry (**B, D**)

3.3.2 Limit of detections

In both µPADs and UV–vis spectrophotometry, the detection limit was determined based on the regression line as *y*-intercept plus three times the standard error (*Sy*/*x*) of the signal (intensity/absorbance in the *y*-direction). The standard error (*Sy*/*x*) of the signal is obtained from the Excel regression output (Miller and Miller 2018). In µPADs method of analysis the limit of detection (LOD) for nitrite and nitrate was found to be 0.16 and 0.87 ppm, respectively. In the case of UV–vis spectrophotometry, it was 0.066 and 0.1 ppm for nitrite and nitrate, respectively. The LOQ in µPADs analysis was 0.53 and 2.91 ppm for nitrite and nitrate, respectively while it was 0.23 and 0.22 ppm for nitrite and nitrate, respectively in the case of UV–vis spectrophotometry analysis. The result indicates that the LOD in µPADs is higher (less sensitive) than the LOD in UV-vis spectrophotometry analysis. Although µ-PADs are less sensitive than UV–vis spectrophotometry in this study, the detection limits obtained for both analytes are below the established regulatory limits, such as 1 ppm for nitrite and 50 ppm for nitrate in drinking water. As it can be seen in Table 1, the µPAD fabricated in this study by wax screen printing method showed a very high sensitivity (LOD = 0.16 ppm) compared with the µ-PAD fabricated by polydimethylsiloxane (PDMS) stamping (LOD = 0.52 ppm) for the analysis of nitrite in drinking water (Lopez-Ruiz et al. 2014).

The LOD reported in this study for nitrite (0.16 ppm) and nitrate (0.87 ppm) offers higher sensitivity than previously reported works (Bhakta et al. 2014; Cardoso et al. 2015; Klasner et al. 2010; Lopez-Ruiz et al. 2014; Teepoo et al. 2019). However, it was found to be less sensitive compared with some of the previous works (Charbaji, et al. 2021a, b; Jayawardane et al. 2014; Ortiz-Gomez et al. 2016; Zhang et al. 2018). In general, the present study demonstrates that the developed µPAD method has adequate sensitivity to evaluate compliance with the maximum permissible limits of nitrite (3 ppm) and nitrate (50 ppm) in drinking water set by the Ethiopian Standard Authority without need for an expensive analytical instrument.

Interference studies

Potential interference from various anions on the µPADs analysis of nitrite and nitrate ions were studied at a concentration of 1 ppm and 10 ppm, respectively. In the presence of Cl^-at concentrations level of 1000, 400, 200, and 50 ppm the analysis of 1 ppm nitrite ion showed percentage recovery of 90.1 (±3.3), 91.7 (±2.5), 96.4 (±2), and 97.7% (±1.7), respectively. And percent recovery over 97% was observed for the analysis of nitrite in the presence of nitrate ion. However, in the presence of CH_3COO^- at concentrations levels of 1000, 400, 200, and 50 ppm, the analysis of 1 ppm nitrite gave percentage recovery of 51.9 (±1.6), 70.3 (±2.3), 75.8 (±1.8), and 86.5 (±2.9), respectively. All the recoveries obtained for the nitrite in the presence

Table 1 Comparison with previously reported μ-PADs for the determination of nitrite and nitrate

Fabrication	Sample matrices	LOD (ppm)	LOQ (ppm)	References
Stamping method (2D)	Ham, sausage and the preservative water from a bottle of Vienna sausage	0.25 (nitrite)	NA	Cardoso et al. (2015)
Paper cutting (2D)	Mineral and tap water	0.06 (nitrite)	0.1	Ortiz-Gomez et al. (2016)
Inkjet printing (3D)	Synthetic, tap, pond and mineral water	0.046 (nitrite)	0.36	Jayawardane et al. (2014)
		1.17 (nitrate)	2.98	
Wax printing (2D)	Saliva	0.40 (nitrite)	NA	Bhakta et al. (2014)
A stamping technique	Water sample	0.52 (nitrite)	NA	Lopez-Ruiz et al. (2014)
Wax	Meat product	1.10 (nitrite)	9.3	Trofimchuk et al. (2020)
Photolithography	Artificial saliva	0.20 (nitrite)	NA	Klasner et al. (2010)
Electrokinetic stacking	Saliva	0.073 (nitrite)	NA	Zhang et al. (2018)
Novel μ-PAD without wax	Human saliva	0.0023 (nitrite)	0.01	Ferreira et al. (2020)
		4.96 (nitrate)	15.5	
Wax printing	Food sample	0.4 (nitrite) 0.4 (nitrate)	NA	Ratnarathorn and Dungchai (2020)
Wax printing	Water sample	0.018 (nitrite)	0.061	Charbaji et al. (2021a, b)
		0.53 (nitrate)	1.765	
Beeswax screen printing method	Food product	0.1 (nitrite)	1.2	Thongkam and Hemavibool (2020)
		0.4 (nitrate)	1.4	
Polylactic acid screen printing	Food sample	1.2 (nitrite)	4	Teepoo et al. (2019)
		3.6 (nitrate)	12	
Wax screen printing	Water sample	0.16 (nitrite)	0.53	This study
		0.87 (nitrate)	2.91	

of Cl^- and NO_3^- ions are in an acceptable range implying that Cl^- and NO_3^- ions don't interfere in the analysis of nitrite. In contrast, the presence of CH_3COO^- significantly drops the recovery of nitrite (below 75%) particularly at a higher concentration level (1000–400 ppm). This result revealed that CH_3COO^- ions significantly affects the analysis of nitrite. Similarly, at 1000 ppm concentration of CH_3COO^-, the recovery for 10 ppm NO^- goes down to 50% implying the potential interference of the CH_3COO^- in the analysis of nitrate as well. However, in the presence of Cl^- (50–1000 ppm), no effect was observed on the analysis of 10 ppm NO_3^-.

3.3.3 Method validation

The nitrite and nitrate ions spiked to tap water were determined using the fabricated μPADs and a UV–visible spectrophotometer. As shown in Table 2, the percentage recovery observed for nitrite was 95–99 and 98–100% in using μPADs and UV–vis spectrophotometry, respectively. Similarly, a nitrate percentage recovery in the range of 96–99% was observed in using μPADs and UV–vis spectrophotometry. This indicates that the μPAD method is in very good agreement with UV–vis spectrophotometry and therefore it could be used for the analysis of nitrite and nitrate in a resource-limited area without a need for an expensive benchtop analytical device.

Table 2 Nitrite and nitrate analysis in spiked tap water samples using μPADs and UV–vis spectrophotometry method

Nitrite analysis in tap water			Nitrate analysis in tap water		
Amount spiked (ppm)	Percentage recovery using μPADs	Percentage recovery using UV–Vis	Amount spiked (ppm)	Percentage recovery using μPADs	Percentage recovery using UV–Vis
0	–	–	0	–	–
0.5	97.38	100.00	4	96.19	96.20
0.6	95.39	98.00	6	97.54	98.27
1	98.74	99.01	8	98.14	98.70
1.2	98.81	100.00	10	99.03	99.67

3.4 Real sample analysis

Groundwater samples collected from Dire Dawa city were analyzed for nitrite ion using both μPAD and UV–vis spectrophotometry. The results revealed that there was no nitrite ion in the groundwater sample. This might not imply absolute zero; perhaps it might be below the detection limit of the analysis method. Therefore, four levels of standard solutions of nitrite were spiked to the groundwater to investigate whether the sample had 0 ppm nitrite or a nitrite level below the detection limit.

Table 3 shows that the actual concentration of nitrite determined by both μPAD and UV–Vis spectrophotometry goes beyond the amount spiked in the groundwater sample. This implies that the groundwater has some amount of nitrite before it was spiked. Based on the μPADs analysis, the average nitrite concentration in the groundwater is calculated to be 0.049 ppm. Likewise, UV–vis spectrophotometry measurement for the nitrite concentration in the groundwater sample also showed 0.05 ppm. Hence, we can conclude from the result that the values obtained from the μPADs and the UV–vis spectrophotometry are in an excellent agreement. In both methods, the amount of the nitrite ion found in the groundwater was 0.05 ppm which is below the detection limit of μPADs and UV–vis spectrophotometry. Furthermore, it is worth to notice that the nitrite concentration in the groundwater sample of Dire Dawa city is below the maximum accepted concentration (MAC) level in drinking water set by US EPA 2009 (1 ppm).

On the other hand, the total nitrate ion concentration in the groundwater sample was found to be 70.53 and 70.60 ppm, using μPADs and UV–vis spectrophotometry, respectively. The deep pink color observed in the μ-PADs image of nitrate (Fig. 9) reveals the high concentration of nitrate in the ground water.

Interestingly, the same concentration of nitrate was also obtained from groundwater by using both μPADs and the UV–Vis method of analysis. This indicates the developed μPADs method of analysis is very reliable for the determination of nitrite and nitrate in various water samples.

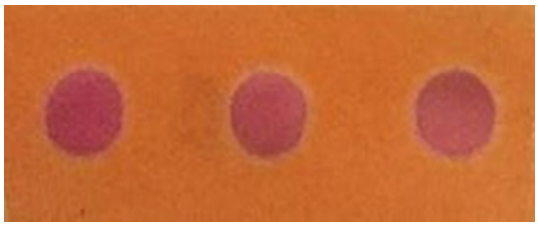

Fig. 9 Colorimetric image for nitrate determination in ground water

This study, besides the analytical method development, revealed that the concentration of nitrate in the groundwater sample (71 ppm) is above the maximum acceptable concentration in drinking water set by both international (WHO, USEPA) and national regulatory body (Ethiopian Standard Agency) which is 50 mg/L (50 ppm).

4 Conclusion

A simple wax screen printing μ-PAD fabrication method affordable to an ordinary laboratory has been demonstrated. The μ-PAD fabricated by this method was used to quantify nitrite and nitrate contamination in water samples and the results were compared and validated with UV–vis spectrophotometric analysis. Excellent agreement was observed between the μ-PAD and UV–vis spectrophotometry results in the nitrite and nitrate analysis of spiked tap-water and groundwater. The detection limits obtained for both analytes are below the established regulatory limits in drinking water. Hence, the developed μ-PAD method could be used to evaluate compliance with the maximum permissible limits of nitrite and nitrate in drinking water set by both international regulatory bodies and the Ethiopian Standard Authority. This study implies that μ-PAD has potential for environmental sample analysis and could substitute or complement conventional analytical instrument-based methodologies, particularly in resource-limited countries. Therefore, microfluidic paper-based analytical devices (μPADs) established

Table 3 The determination of nitrite in groundwater samples

Nitrite analysis using μPADs			Nitrite analysis using UV–vis spectrophotometry	
Amount spiked in ppm (A_0)	Actually determined (A_f)	Difference (A_f–A_0)	Actually determined (A_f)	Difference (A_f–A_0)
0	0	0	0	0
0.5	0.5477	0.0477	0.5494	0.0494
0.6	0.6487	0.0487	0.6492	0.0492
1.0	1.0499	0.0499	1.0501	0.0501
1.2	1.2500	0.05	1.2503	0.0503
Average difference		0.049 ppm	Average difference	0.05 ppm

in this study has a significant contribution towards realizing the ASSURED policy set by WHO. Furthermore, the study revealed the nitrate concentration found in the groundwater sample (71 ppm) was above the maximum acceptable concentration in drinking water, which needs attention by the concerned body to explore on some treatment techniques to reduce the nitrate concentration to the acceptable level.

Acknowledgements The authors thank Addis Ababa University Thematic Research Fund for supporting the project entitled "Developing Innovative Microfluidic Paper-Based Analytical Devices (μ-PADs): Viable solution for Environmental Monitoring in Ethiopia" at the Centre for Environmental Science. The authors also acknowledge Dawit Firemichael, Gizachew Wendimu and Dr. Yedilfana Setarge for their assistance in editing the manuscript.

Author contributions TT performed the experiment, analyzed the data and prepared zero draft of the manuscript. AH contributed to the conception of the study, methodology analyzed the data and wrote the manuscript.

Funding Addis Ababa University, Thematic Research Fund by the office of the Vice President for Research and Technology Transfer (VPRTT/PY-021/2018/10).

Availability of data and materials The data sets supporting the results of this article are included within the article and supplementary materials.

Code availability N/A.

Declarations

Conflict of interest The authors declared that they have no competing interests.

References

Acrylamide O (2009) National primary drinking water regulations. Kidney 2(4-D):0.07

Bhakta SA, Borba R, Taba M Jr, Garcia CD, Carrilho E (2014) Determination of nitrite in saliva using microfluidic paper-based analytical devices. Anal Chim Acta 809:117–122

Bhatnagar A, Sillanpää M (2009) Applications of chitin-and chitosan-derivatives for the detoxification of water and wastewater—a short review. Adv Coll Interface Sci 152(1–2):26–38

Bruning-Fann CS, Kaneene J (1993) The effects of nitrate, nitrite and *N*-nitroso compounds on human health: a review. Vet Hum Toxicol 35(6):521–538

Cardoso TM, Garcia PT, Coltro WK (2015) Colorimetric determination of nitrite in clinical, food and environmental samples using microfluidic devices stamped in paper platforms. Anal Methods 7(17):7311–7317

Charbaji A, Heidari-Bafroui H, Anagnostopoulos C, Faghri M (2021a) A new paper-based microfluidic device for improved detection of nitrate in water. Sensors 21(1):102

Charbaji A, Smith W, Anagnostopoulos C, Faghri M (2021b) Zinculose: a new fibrous material with embedded zinc particles. Eng Sci Technol 24(2):571–578

Chiu H-F, Tsai S-S, Yang C-Y (2007) Nitrate in drinking water and risk of death from bladder cancer: an ecological case-control study in Taiwan. J Toxicol Environ Health A 70(12):1000–1004

Dungchai W, Chailapakul O, Henry CS (2011) A low-cost, simple, and rapid fabrication method for paper-based microfluidics using wax screen-printing. Analyst 136(1):77–82

Ferreira FT, Mesquita RB, Rangel AO (2020) Novel microfluidic paper-based analytical devices (μPADs) for the determination of nitrate and nitrite in human saliva. Talanta 219:121183

Jayawardane BM, Wei S, McKelvie ID, Kolev SD (2014) Microfluidic paper-based analytical device for the determination of nitrite and nitrate. Anal Chem 86(15):7274–7279

Klasner SA, Price AK, Hoeman KW, Wilson RS, Bell KJ, Culbertson CT (2010) based microfluidic devices for analysis of clinically relevant analytes present in urine and saliva. Anal Bioanal Chem 397(5):1821–1829

Kostraba JN, Gay EC, Rewers M, Hamman RF (1992) Nitrate levels in community drinking waters and risk of IDDM: an ecological analysis. Diabetes Care 15(11):1505–1508

Limousy L, Dutournie P, Hadjiev D (2010) Kinetics of nitrite reduction by zinc metal: influence of metal shape on the determination of kinetic parameters. Water Environ Res 82(7):648–656

Lopez-Ruiz N, Curto VF, Erenas MM, Benito-Lopez F, Diamond D, Palma AJ, Capitan-Vallvey LF (2014) Smartphone-based simultaneous pH and nitrite colorimetric determination for paper microfluidic devices. Anal Chem 86(19):9554–9562

Martinez AW, Phillips ST, Whitesides GM, Carrilho E (2010) Diagnostics for the developing world: microfluidic paper-based analytical devices. ACS Publications, Washington

Mikuška P, Večeřa Z (2003) Simultaneous determination of nitrite and nitrate in water by chemiluminescent flow-injection analysis. Anal Chim Acta 495(1–2):225–232

Miller J, Miller JC (2018) Statistics and chemometrics for analytical chemistry. Pearson Education, London

Murray E, Nesterenko EP, McCaul M, Morrin A, Diamond D, Moore B (2017) A colorimetric method for use within portable test kits for nitrate determination in various water matrices. Anal Methods 9(4):680–687

Narayana B, Sunil K (2009) A spectrophotometric method for the determination of nitrite and nitrate. Euras J Anal Chem 4(2):204–214

Nishat S, Jafry AT, Martinez AW, Awan FR (2021) Based microfluidics: simplified fabrication and assay methods. Sens Actuators B Chem 336:129681

Ortiz-Gomez I, Ortega-Muñoz M, Salinas-Castillo A, Álvarez-Bermejo JA, Ariza-Avidad M, de Orbe- Payá I, Capitan-Vallvey LF (2016) Tetrazine-based chemistry for nitrite determination in a paper microfluidic device. Talanta 160:721–728

Pereira EA, Petruci JF, Cardoso AA (2012) Determination of nitrite and nitrate in Brazilian meats using high shear homogenization. Food Anal Methods 5(4):637–642

Pistón M, Mollo A, Knochen M (2011) A simple automated method for the determination of nitrate and nitrite in infant formula and milk powder using sequential injection analysis. J Autom Methods Manag Chem 2011:1–7

Ratnarathorn N, Dungchai W (2020) Based analytical device (PAD) for the determination of borax, salicylic acid, nitrite, and nitrate by colorimetric methods. J Anal Chem 75(4):487–494

Rezaee A, Godini H, Dehestani S, Khavanin A (2008) Application of impregnated almond shell activated carbon by zinc and zinc sulfate for nitrate removal from water. J Environ Health Sci Eng 5(2):125–130

Teepoo S, Arsawiset S, Chanayota P (2019) One-step polylactic acid screen-printing microfluidic paper- based analytical device: application for simultaneous detection of nitrite and nitrate in food samples. Chemosensors 7(3):44

Thongkam T, Hemavibool K (2020) An environmentally friendly microfluidic paper-based analytical device for simultaneous colorimetric detection of nitrite and nitrate in food products. Microchem J 159:105412

Trofimchuk E, Hu Y, Nilghaz A, Hua MZ, Sun S, Lu X (2020) Development of paper-based microfluidic device for the determination of nitrite in meat. Food Chem 316:126396

van Breda SG, Mathijs K, Sági-Kiss V, Kuhnle GG, Van der Veer B, Jones RR, de Kok TM (2019) Impact of high drinking water nitrate levels on the endogenous formation of apparent N-nitroso compounds in combination with meat intake in healthy volunteers. Environ Health 18(1):1–12

Ward MH, Jones RR, Brender JD, De Kok TM, Weyer PJ, Nolan BT, Van Breda SG (2018) Drinking water nitrate and human health: an updated review. Int J Environ Res Public Health 15(7):1557

Zhang X-X, Song Y-Z, Fang F, Wu Z-Y (2018) Sensitive paper-based analytical device for fast colorimetric detection of nitrite with smartphone. Anal Bioanal Chem 410(11):2665–2669